



Effect of electrolyte addition on activity of $(\text{Ga}_{1-x}\text{Zn}_x)(\text{N}_{1-x}\text{O}_x)$ photocatalyst for overall water splitting under visible light

Kazuhiko Maeda¹, Hideaki Masuda, Kazunari Domen^{*}

Department of Chemical System Engineering, The University of Tokyo, 7-3-1 Hongo, Bunkyo-ku, Tokyo 113-8656, Japan

ARTICLE INFO

Article history:

Available online 31 October 2008

Keywords:

Electrolyte
Hydrogen production
Overall water splitting
Seawater
Solar energy conversion
Visible light

ABSTRACT

Effects of electrolyte addition on photocatalytic activity of $(\text{Ga}_{1-x}\text{Zn}_x)(\text{N}_{1-x}\text{O}_x)$ modified with either $\text{Rh}_{2-y}\text{Cr}_y\text{O}_3$ or RuO_2 nanoparticles as cocatalysts for overall water splitting under visible light ($\lambda > 400 \text{ nm}$) are investigated. The cocatalyst $\text{Rh}_{2-y}\text{Cr}_y\text{O}_3$ is confirmed to selectively promote the photoreduction of H^+ , while RuO_2 functions as both H_2 evolution sites and as efficient O_2 evolution sites. The activity of $\text{Rh}_{2-y}\text{Cr}_y\text{O}_3$ -loaded $(\text{Ga}_{1-x}\text{Zn}_x)(\text{N}_{1-x}\text{O}_x)$ is found to be suppressed in the presence of Cl^- , which undergoes oxidation by photogenerated holes in the valence band of $(\text{Ga}_{1-x}\text{Zn}_x)(\text{N}_{1-x}\text{O}_x)$. Alkaline- and alkaline earth-metal cations in the reactant solution compensate the negative effect of Cl^- to a certain extent depending on the metal cation employed. Among the electrolytes examined, the addition of an appropriate amount of NaCl or A_2SO_4 ($\text{A} = \text{Li}, \text{Na}, \text{or K}$) to the reactant solution without pH control is found to increase activity by up to 75% compared to the case without additives. Direct splitting of seawater to produce H_2 and O_2 is also demonstrated using $\text{Rh}_{2-y}\text{Cr}_y\text{O}_3$ -loaded $(\text{Ga}_{1-x}\text{Zn}_x)(\text{N}_{1-x}\text{O}_x)$ catalyst under visible light.

© 2008 Elsevier B.V. All rights reserved.

1. Introduction

Photocatalytic overall water splitting using a heterogeneous photocatalyst has been studied extensively as a potential method to supply hydrogen from sunlight and water [1–4]. From the viewpoint of practical application, the ability to produce hydrogen from natural seawater, the most abundant water resource, would be highly desirable. However, natural seawater contains a range of inorganic cations and anions, and the effects of such ions on the activity of the water splitting reaction remains to be investigated in more detail. Lee and co-workers recently reported that the overall water splitting using NiO_x -loaded $\text{La}_2\text{Ti}_2\text{O}_7$ under ultraviolet (UV) irradiation ($\lambda > 200 \text{ nm}$) can be achieved in seawater, although at half the rate of activity compared to that in pure water [5]. It was concluded that the suppression of activity in seawater is mainly attributable to the presence of magnesium cations in the reactant solution. The visible light photocatalytic activity of a platinum-loaded CdS/TiO_2 composite catalyst for H_2 evolution in the presence of SO_3^{2-} and S^{2-} as sacrificial electron donors and an Fe_2O_3 thin-film electrode for anodic photocurrent generation was also investigated in that study using seawater. However, there are

as yet no studies on the activity of visible light-driven photocatalysts for overall water splitting in seawater.

Our group has reported that the $(\text{Ga}_{1-x}\text{Zn}_x)(\text{N}_{1-x}\text{O}_x)$ solid solution is a stable photocatalyst for overall water splitting under visible light ($\lambda > 400 \text{ nm}$), when modified with an appropriate cocatalyst to promote H_2 evolution [6–14]. The photocatalytic activity of $(\text{Ga}_{1-x}\text{Zn}_x)(\text{N}_{1-x}\text{O}_x)$ for overall water splitting has been examined with respect to the physicochemical properties of $(\text{Ga}_{1-x}\text{Zn}_x)(\text{N}_{1-x}\text{O}_x)$ [7], the cocatalyst [8–13], and the pH of the reactant solution [14]. The highest activity for overall water splitting achieved by this photocatalytic system has been obtained using $(\text{Ga}_{1-x}\text{Zn}_x)(\text{N}_{1-x}\text{O}_x)$ modified with nanoparticulate Rh–Cr mixed oxide ($\text{Rh}_{2-y}\text{Cr}_y\text{O}_3$) in aqueous H_2SO_4 solution at pH 4.5 [14]. However, the effect of inorganic ions in the reactant solution on the activity of this catalyst has not been investigated.

In this paper, the effects of various electrolytes on the activity of $\text{Rh}_{2-y}\text{Cr}_y\text{O}_3$ - and RuO_2 -loaded $(\text{Ga}_{1-x}\text{Zn}_x)(\text{N}_{1-x}\text{O}_x)$ for overall water splitting under visible light ($\lambda > 400 \text{ nm}$) are investigated, and the direct splitting of seawater using $\text{Rh}_{2-y}\text{Cr}_y\text{O}_3$ -loaded $(\text{Ga}_{1-x}\text{Zn}_x)(\text{N}_{1-x}\text{O}_x)$ is attempted.

2. Experimental

2.1. Preparation of catalysts

The $(\text{Ga}_{1-x}\text{Zn}_x)(\text{N}_{1-x}\text{O}_x)$ solid solution was prepared according to the method presented in previous papers [6,7]. Briefly, a mixture

^{*} Corresponding author. Tel.: +81 3 5841 1148; fax: +81 3 5841 8838.

E-mail address: domen@chemsys.t.u-tokyo.ac.jp (K. Domen).

¹ Research Fellow of the Japan Society for the Promotion of Science (JSPS).

of Ga_2O_3 and ZnO powders (1.08 g Ga_2O_3 and 0.94 g ZnO) was heated at 1123 K under NH_3 flow (250 mL min^{-1}). After 15 h of nitridation, the sample was cooled to room temperature under NH_3 flow. The production of $(\text{Ga}_{1-x}\text{Zn}_x)(\text{N}_{1-x}\text{O}_x)$ with $x = 0.12$ was confirmed by powder X-ray diffraction (XRD) and energy-dispersive X-ray analysis (EDX). The band-gap energy of the as-obtained $(\text{Ga}_{1-x}\text{Zn}_x)(\text{N}_{1-x}\text{O}_x)$ is 2.68 eV, as estimated from the onset of the diffuse reflectance spectrum.

Nanoparticulate $\text{Rh}_{2-y}\text{Cr}_y\text{O}_3$ or RuO_2 was loaded as a cocatalyst onto the as-prepared $(\text{Ga}_{1-x}\text{Zn}_x)(\text{N}_{1-x}\text{O}_x)$ according to the method described previously [7–11,14]. Rhodium and chromium were loaded at rates of 1 and 1.5 wt% (metallic content), respectively [11]. The RuO_2 loading achieved in this manner was 5 wt% [10].

2.2. Photocatalytic reactions

Reactions were carried out in a Pyrex inner-irradiation-type reaction vessel connected to a glass closed gas circulation system. Electrolytes of reagent grade were purchased and used as received. A 0.3-g sample of the cocatalyst-loaded catalyst powder was dispersed in various reactant solutions (370–400 mL) containing a range of electrolytes. Artificial seawater was prepared by dissolving a series of electrolytes (NaCl , 28.5 g; $\text{MgSO}_4 \cdot 7\text{H}_2\text{O}$, 6.82 g; $\text{MgCl}_2 \cdot 6\text{H}_2\text{O}$, 5.16 g; $\text{CaCl}_2 \cdot 2\text{H}_2\text{O}$, 1.47 g; KCl , 0.725 g; $\text{SrCl}_2 \cdot 6\text{H}_2\text{O}$, 0.024 g; NaBr , 0.084 g; H_3BO_3 , 0.0273 g; NaF , 2.9 mg; KI , 0.1 mg) in 1000 mL of distilled water. The reactant solution was first evacuated several times to ensure complete air removal, and then irradiated under a 450-W high-pressure mercury lamp via a Pyrex tube filled with aqueous NaNO_2 solution (2 M) as a filter to block UV light ($\lambda > 400 \text{ nm}$). The reactant solution was maintained at room temperature by a flow of cooling water during the reaction. The evolved gases were analyzed by gas chromatography. The experimental error of activity tests in the present study is within 10%.

3. Results and discussion

3.1. Reactivities of $\text{Rh}_{2-y}\text{Cr}_y\text{O}_3$ - and RuO_2 -loaded $(\text{Ga}_{1-x}\text{Zn}_x)(\text{N}_{1-x}\text{O}_x)$

Table 1 lists the rates of H_2 and O_2 evolution (average over 5 h) in overall water splitting using $\text{Rh}_{2-y}\text{Cr}_y\text{O}_3$ - and RuO_2 -loaded $(\text{Ga}_{1-x}\text{Zn}_x)(\text{N}_{1-x}\text{O}_x)$ under visible light ($\lambda > 400 \text{ nm}$) from various aqueous solutions. The pH of the solutions was adjusted by the reagent shown. As reported previously, the optimal reaction pH for overall water splitting is 4.5 for $\text{Rh}_{2-y}\text{Cr}_y\text{O}_3$ -loaded $(\text{Ga}_{1-x}\text{Zn}_x)(\text{N}_{1-x}\text{O}_x)$ and 3.0 for the RuO_2 -loaded catalyst (when adjusted with H_2SO_4), with both catalysts exhibiting steady and stoichiometric H_2 and O_2 evolution [6,14]. The

present reactions were therefore carried out at these pH respective levels. The $\text{Rh}_{2-y}\text{Cr}_y\text{O}_3$ -loaded $(\text{Ga}_{1-x}\text{Zn}_x)(\text{N}_{1-x}\text{O}_x)$ produced H_2 and O_2 steadily and stoichiometrically (i.e., overall water splitting) regardless of the pH-adjusting reagent employed. Almost identical activity was obtained when the pH was adjusted using H_2SO_4 (entry 1) and HNO_3 (entry 2). However, the use of HCl as the pH-adjusting reagent resulted in an approximately 60% drop in activity (entry 3) compared to the reactions performed using H_2SO_4 (entry 1) or HNO_3 (entry 2). In contrast, RuO_2 -loaded $(\text{Ga}_{1-x}\text{Zn}_x)(\text{N}_{1-x}\text{O}_x)$ displayed almost the same activity in aqueous HCl solution (entry 6) as in aqueous H_2SO_4 solution (entry 4), although stoichiometric H_2 and O_2 evolution was not achieved over any period of reaction when the reaction pH was adjusted using HNO_3 (entry 5). As revealed in a previous study, the higher activity of $\text{Rh}_{2-y}\text{Cr}_y\text{O}_3$ -loaded $(\text{Ga}_{1-x}\text{Zn}_x)(\text{N}_{1-x}\text{O}_x)$ in aqueous H_2SO_4 solution compared to the RuO_2 -loaded catalyst is attributable to the superior H_2 evolution ability of $\text{Rh}_{2-y}\text{Cr}_y\text{O}_3$ and the inhibition of O_2 photoreduction (a backward reaction in photocatalytic overall water splitting) [14]. It was found in the present study that the photocatalytic activity of $(\text{Ga}_{1-x}\text{Zn}_x)(\text{N}_{1-x}\text{O}_x)$ for overall water splitting is dependent not only on the cocatalyst employed but also on the reagent used to adjust the pH. A negligible amount of N_2 evolution (ca. 5–10 μmol) was detected in the initial stage of the reaction (first 1–2 h) in all cases, attributable to the oxidation of N^{3-} species near the $(\text{Ga}_{1-x}\text{Zn}_x)(\text{N}_{1-x}\text{O}_x)$ surface to N_2 [14], as has been observed for other (oxy)nitride photocatalysts [4]. However, the production of N_2 was completely suppressed as the reaction proceeded.

These characteristic gas evolution properties can be explained in terms of the different reactivities of each catalyst with respect to redox-active species in the aqueous solution. Inorganic ions can react with photogenerated electrons and/or holes on photocatalysts, thereby inhibiting the efficiency of overall water splitting, which is primarily dependent on the redox potential of ions and the band-edge positions of the photocatalyst. Photoelectrochemical measurements using a porous $(\text{Ga}_{1-x}\text{Zn}_x)(\text{N}_{1-x}\text{O}_x)$ anode suggest that the bottom of the conduction band of $(\text{Ga}_{1-x}\text{Zn}_x)(\text{N}_{1-x}\text{O}_x)$ lies at ca. -0.92 V vs. NHE (at pH 4.5) [15]. Accordingly, electrons photogenerated in the conduction band of $(\text{Ga}_{1-x}\text{Zn}_x)(\text{N}_{1-x}\text{O}_x)$ are unable to reduce SO_4^{2-} to SO_3^{2-} thermodynamically, since the thermodynamic reduction potential of SO_4^{2-} ($\text{SO}_4^{2-}/\text{SO}_3^{2-}$, -1.22 V vs. NHE at pH 4.5) is more negative than the conduction band bottom of $(\text{Ga}_{1-x}\text{Zn}_x)(\text{N}_{1-x}\text{O}_x)$ [16]. Therefore, the reduction of SO_4^{2-} by $(\text{Ga}_{1-x}\text{Zn}_x)(\text{N}_{1-x}\text{O}_x)$ does not take place.

NO_3^- , which is more susceptible to reduction than H^+ ($\text{NO}_3^-/\text{NO}_2^-$, $+0.54 \text{ V}$; H^+/H_2 , -0.27 V vs. NHE at pH 4.5) [16], can compete with the reduction of H^+ by conduction band electrons, thereby lowering the overall water splitting activity. It has been reported that NO_3^- can be catalytically reduced during the water splitting reaction when using a semiconductor photocatalyst [17]. The non-stoichiometric evolution of H_2 and O_2 by the RuO_2 -loaded catalyst in HNO_3 solution (entry 5) is thus attributable to the competition between the reduction of NO_3^- and the reduction of H^+ to H_2 . Analysis of the reactant solution by ion chromatography indicates that NO_2^- and NH_3 are generated as reaction products in the reaction over RuO_2 -loaded $(\text{Ga}_{1-x}\text{Zn}_x)(\text{N}_{1-x}\text{O}_x)$. In contrast, the reduction of NO_3^- does not appear to occur over the $\text{Rh}_{2-y}\text{Cr}_y\text{O}_3$ -loaded catalyst, as indicated by the similarity of the overall water splitting activity for the HNO_3 (entry 2) and H_2SO_4 (entry 1) solutions and the stoichiometric ratio of H_2 to O_2 evolution achieved using this system (Table 1). It was also confirmed that the H_2/O_2 evolution ratio remains stoichiometric even in the presence of 10 mM NO_3^- (pH 4.5), although the absolute rates of gas evolution are 10–15% lower.

Table 1

Photocatalytic activities of $(\text{Ga}_{1-x}\text{Zn}_x)(\text{N}_{1-x}\text{O}_x)$ -loaded with $\text{Rh}_{2-y}\text{Cr}_y\text{O}_3$ or RuO_2 for overall water splitting under visible light ($\lambda > 400 \text{ nm}$) in aqueous solutions (pH 4.5 or 3.0) containing either H_2SO_4 , HNO_3 or HCl^a .

Entry	Cocatalyst	pH	Reagent	Activity ^b ($\mu\text{mol h}^{-1}$)	
				H_2	O_2
1	$\text{Rh}_{2-y}\text{Cr}_y\text{O}_3$	4.5	H_2SO_4	264	132
2			HNO_3	255	127
3			HCl	166	83
4	RuO_2	3.0	H_2SO_4	58	29
5			HNO_3	6.7	24
6			HCl	60	30

^a Reaction conditions: catalyst, 0.3 g; reaction solution, aqueous solution (370–400 mL); light source, high-pressure mercury lamp (450 W); reaction vessel, Pyrex inner-irradiation vessel with aqueous NaNO_2 solution filter.

^b Average rate of gas evolution for 5 h.

This result indicates that the photoreduction of NO_3^- over $\text{Rh}_{2-y}\text{Cr}_y\text{O}_3$ -loaded $(\text{Ga}_{1-x}\text{Zn}_x)(\text{N}_{1-x}\text{O}_x)$ proceeds very slowly compared to the reduction of H^+ . Furthermore, previous experiments have revealed that the steady rate of H_2 evolution in overall water splitting by $\text{Rh}_{2-y}\text{Cr}_y\text{O}_3$ -loaded $(\text{Ga}_{1-x}\text{Zn}_x)(\text{N}_{1-x}\text{O}_x)$ remains unchanged even in the presence of oxygen (an electron acceptor) at a partial pressure of up to 30 kPa [14]. These results provide strong evidence that the $\text{Rh}_{2-y}\text{Cr}_y\text{O}_3$ cocatalyst possesses excellent selectivity for the reduction of H^+ to H_2 .

Another difference between these two catalysts is the drop in activity of $\text{Rh}_{2-y}\text{Cr}_y\text{O}_3$ -loaded $(\text{Ga}_{1-x}\text{Zn}_x)(\text{N}_{1-x}\text{O}_x)$ in HCl-adjusted solution (entry 3), whereas the activity of the RuO_2 -loaded catalyst using HCl (entry 6) remained similar to that the H_2SO_4 -adjusted solution (entries 1 and 4). Chloride ions in the reactant solution thus appear to have a negative effect on the activity of $\text{Rh}_{2-y}\text{Cr}_y\text{O}_3$ -loaded $(\text{Ga}_{1-x}\text{Zn}_x)(\text{N}_{1-x}\text{O}_x)$, but not on the RuO_2 -loaded catalyst. In the case of $\text{Rh}_{2-y}\text{Cr}_y\text{O}_3$ -loaded $(\text{Ga}_{1-x}\text{Zn}_x)(\text{N}_{1-x}\text{O}_x)$, water reduction takes place on $\text{Rh}_{2-y}\text{Cr}_y\text{O}_3$ nanoparticles and oxidation occurs on $(\text{Ga}_{1-x}\text{Zn}_x)(\text{N}_{1-x}\text{O}_x)$ [14]. Although the oxidation of Cl^- is thermodynamically more difficult than the oxidation of H_2O (Cl_2/Cl^- , 1.39 V; $\text{O}_2/\text{H}_2\text{O}$, 0.96 V vs. NHE at pH 4.5) [16], the photooxidation of Cl^- to Cl_2 involves a relatively simple 2-electron redox process and is thus likely to proceed more readily than the photooxidation of H_2O to O_2 , which involves a complex 4-electron redox process. If Cl_2 is produced as a result of the photooxidation of Cl^- in photocatalytic overall water splitting, the ratio of H_2 to O_2 evolution should become larger than that expected from the stoichiometry (i.e., $\text{H}_2/\text{O}_2 = 2$) at the normal rate of H_2 evolution. However, the ratio of H_2 to O_2 evolution over $\text{Rh}_{2-y}\text{Cr}_y\text{O}_3$ -loaded $(\text{Ga}_{1-x}\text{Zn}_x)(\text{N}_{1-x}\text{O}_x)$ in aqueous HCl solution satisfies the stoichiometry (entry 3), with the rates of both H_2 and O_2 evolution obviously lower than in the H_2SO_4 -adjusted solution (entry 1). The concentration of HCl in the solution (pH 4.5) is approximately 0.03 mM, corresponding to 12 $\mu\text{mol Cl}^-$. Assuming that all of the Cl^- in the solution undergoes oxidation to produce Cl_2 , the maximum rate of Cl_2 production is only 1.2 $\mu\text{mol h}^{-1}$ (average over 5 h), which is much lower than the observed rate of O_2 evolution. Competitive Cl_2 production therefore does not appear to affect the rate of O_2 evolution. The stoichiometry of the H_2/O_2 ratio would thus be maintained even if the photooxidation of Cl^- proceeds in this system. Given this situation, the suppression of the rates of H_2 and O_2 evolution in the HCl-adjusted solution indicates that solvated Cl^- in the reactant solution hinders not only water oxidation but also water reduction. Although the detailed action of Cl^- in this reaction is not well understood, one possible explanation is the reduction by photogenerated electrons of intermediates produced by the photooxidation of Cl^- . Such a process would result in lower water reduction activity, and explains the simultaneous suppression of the rates of both H_2 and O_2 evolution while maintaining stoichiometry. There are some reports describing a negative effect of Cl^- on photocatalytic oxidation of organic compounds, which are claimed to be attributable to hindrance of active sites in the catalyst surface by adsorption of Cl^- [18,19]. In contrast, the fact that the activity of RuO_2 -loaded $(\text{Ga}_{1-x}\text{Zn}_x)(\text{N}_{1-x}\text{O}_x)$ in an aqueous HCl solution is almost the same (entry 6) as that in an aqueous H_2SO_4 solution (entry 4) indicates that there is no negative effect of Cl^- , and implies that oxidation of Cl^- does not take place on this catalyst. RuO_2 is well known as a good oxidation catalyst for O_2 evolution. In the case of water splitting, RuO_2 has been demonstrated by many researchers to be effective as an oxidation site for the evolution of O_2 [20–24]. In the $(\text{Ga}_{1-x}\text{Zn}_x)(\text{N}_{1-x}\text{O}_x)$, however, the primary role of nanoparticulate RuO_2 is to provide catalytic active sites for H_2 evolution [14].

It therefore appears that nanoparticulate RuO_2 functions as both an H_2 evolution site and an efficient O_2 evolution site in the presence of Cl^- .

3.2. Effect of anions on activity

As shown in Table 1, Cl^- in aqueous solution has a negative effect on the activity of $\text{Rh}_{2-y}\text{Cr}_y\text{O}_3$ -loaded $(\text{Ga}_{1-x}\text{Zn}_x)(\text{N}_{1-x}\text{O}_x)$ in overall water splitting. To obtain more information regarding this effect of Cl^- , the concentration of Cl^- in the reactant solution was varied. Fig. 1 shows the dependence of the rates of H_2 and O_2 evolution (average over 5 h) in overall water splitting using $\text{Rh}_{2-y}\text{Cr}_y\text{O}_3$ -loaded $(\text{Ga}_{1-x}\text{Zn}_x)(\text{N}_{1-x}\text{O}_x)$ under visible light ($\lambda > 400 \text{ nm}$) on the concentration of NaCl in the reactant solution. Although the reactions were performed without pH control (pH 5.3–6.3), the photocatalytic performance of $\text{Rh}_{2-y}\text{Cr}_y\text{O}_3$ -loaded $(\text{Ga}_{1-x}\text{Zn}_x)(\text{N}_{1-x}\text{O}_x)$ for overall water splitting in the initial stage of the reaction (5 h) is relatively constant in the pH range of this reaction [14]. The rates of H_2 and O_2 evolution increased with NaCl concentration to a maximum at 5 mM, beyond which the evolution rates began to decrease significantly. The ratio of evolved H_2 to O_2 also tended to increase beyond the stoichiometric value of 2 with increasing NaCl concentration. Fig. 2 shows the time courses of H_2 and O_2 evolution using $\text{Rh}_{2-y}\text{Cr}_y\text{O}_3$ -loaded $(\text{Ga}_{1-x}\text{Zn}_x)(\text{N}_{1-x}\text{O}_x)$ in the presence of NaCl. Regardless of the NaCl concentration, steady H_2 and O_2 evolution was observed, indicating no deactivation of catalytic

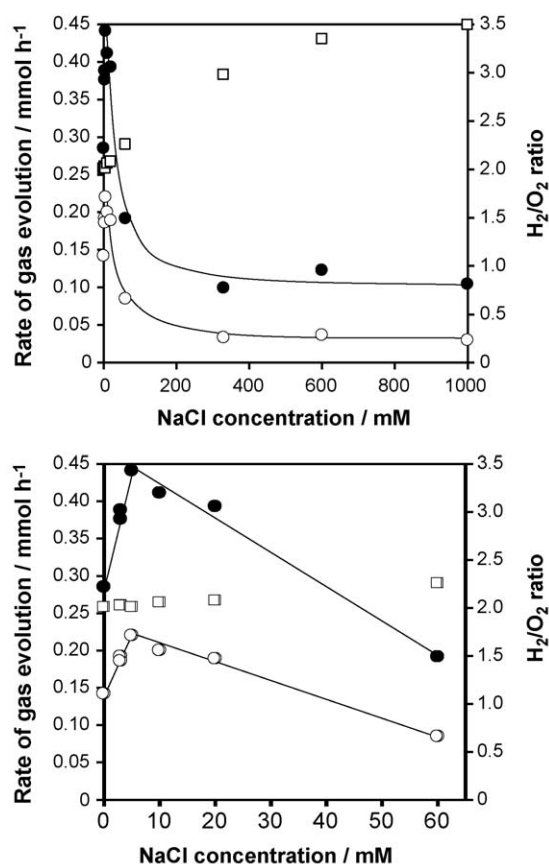


Fig. 1. Dependence of rate of H_2 and O_2 evolution in overall water splitting using $\text{Rh}_{2-y}\text{Cr}_y\text{O}_3$ -loaded $(\text{Ga}_{1-x}\text{Zn}_x)(\text{N}_{1-x}\text{O}_x)$ under visible light ($\lambda > 400 \text{ nm}$) on NaCl concentration. Reaction conditions: catalyst, 0.3 g; reaction solution, 400 mL; light source, high-pressure mercury lamp (450 W); reaction vessel, Pyrex inner-irradiation vessel with aqueous NaNO_2 solution filter. Solid circles, H_2 ; open circles, O_2 ; open squares, H_2/O_2 evolution ratio. Top and bottom panels show different ranges of NaCl concentration.

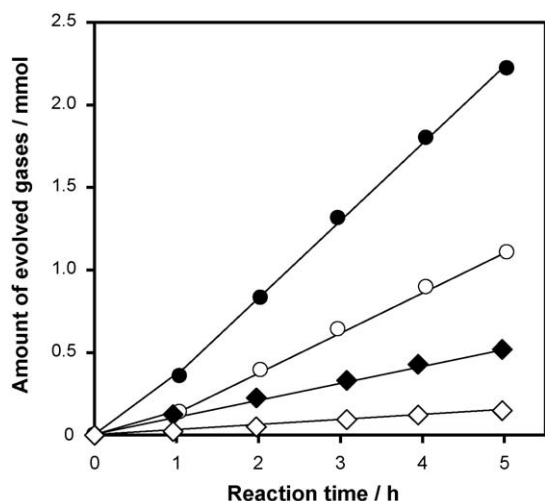


Fig. 2. Time courses of H_2 and O_2 evolution using $\text{Rh}_{2-y}\text{Cr}_y\text{O}_3$ -loaded $(\text{Ga}_{1-x}\text{Zn}_x)(\text{N}_{1-x}\text{O}_x)$ under visible light ($\lambda > 400 \text{ nm}$) in the presence of NaCl. Reaction conditions: catalyst, 0.3 g; reaction solution, 400 mL; light source, high-pressure mercury lamp (450 W); reaction vessel, Pyrex inner-irradiation vessel with aqueous NaNO_2 solution filter. Solid circles, H_2 (5 mM NaCl); open circles, O_2 (5 mM NaCl); solid squares, H_2 (1000 mM NaCl); open squares, O_2 (1000 mM NaCl).

activity with reaction time even in the presence of high concentrations of NaCl.

The experimental results clearly indicate that, except for the low concentration region, overall water splitting (i.e., stoichiometric H_2 and O_2 evolution) is suppressed by the presence of NaCl in the reactant solution. Furthermore, judging from the deviation of the H_2/O_2 ratio from stoichiometry, Cl^- in the reactant solution appears to be oxidized by a fraction of the photogenerated holes in the valence band of $(\text{Ga}_{1-x}\text{Zn}_x)(\text{N}_{1-x}\text{O}_x)$. It was also confirmed by ion chromatography that oxidation products of Cl^- , such as ClO_3^- , are present in the solution after the reaction, although at much lower concentrations than the concentration of Cl^- remaining in the reactant solution. Interestingly, this behavior differs from that observed for the previously reported NiO_x -loaded $\text{La}_2\text{Ti}_2\text{O}_7$ catalyst, which displays no activity for the oxidation of Cl^- [4]. Presumably, the nature of active sites for the photooxidation reaction is different in each case, reflecting the unique photocatalytic properties of each material.

It is also notable that the activity of $\text{Rh}_{2-y}\text{Cr}_y\text{O}_3$ -loaded $(\text{Ga}_{1-x}\text{Zn}_x)(\text{N}_{1-x}\text{O}_x)$ at neutral pH (6) does not decrease even in the presence of up to 20 mM Cl^- , whereas at slightly acidic pH (4.5), the activity decreased by approximately 60% even in the presence of a small amount of Cl^- (ca. 0.03 mM), as shown in Table 1. These results suggest that the negative effect of Cl^- on the overall water splitting activity of $\text{Rh}_{2-y}\text{Cr}_y\text{O}_3$ -loaded $(\text{Ga}_{1-x}\text{Zn}_x)(\text{N}_{1-x}\text{O}_x)$ is more pronounced under acidic pH conditions than under neutral conditions, and/or that the counter cation (in this case, Na^+) compensates for the negative effect of Cl^- under neutral conditions to maintain activity. This possibility was investigated by performing reaction in aqueous H_2SO_4 solution (pH 4.5) with and without 10 mM NaCl. Fig. 3 shows the time courses of overall water splitting using the $\text{Rh}_{2-y}\text{Cr}_y\text{O}_3$ -loaded $(\text{Ga}_{1-x}\text{Zn}_x)(\text{N}_{1-x}\text{O}_x)$ catalyst with and without 10 mM NaCl at pH 6.3 and 4.5. In contrast to the increase in activity observed at pH 6.3 (also as shown in Fig. 1), the addition of NaCl to the reactant solution at pH 4.5 did not lead to any appreciable increase in activity. This result indicates that the detrimental effect of Cl^- is to some extent pronounced under acidic pH condition. Nevertheless, the activity at pH 4.5 in the presence of 10 mM NaCl (H_2 , $300 \mu\text{mol h}^{-1}$; O_2 , $143 \mu\text{mol h}^{-1}$) is clearly improved compared to

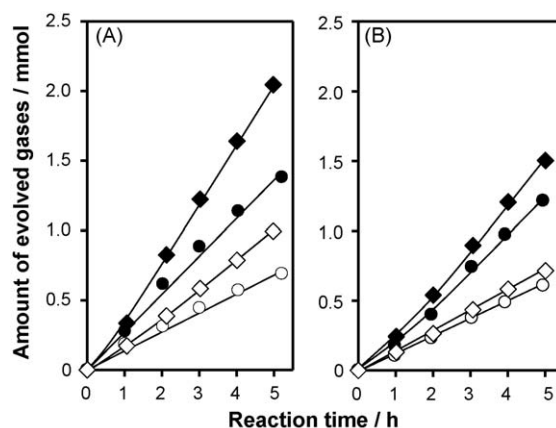


Fig. 3. Time courses of H_2 and O_2 evolution using $\text{Rh}_{2-y}\text{Cr}_y\text{O}_3$ -loaded $(\text{Ga}_{1-x}\text{Zn}_x)(\text{N}_{1-x}\text{O}_x)$ under visible light ($\lambda > 400 \text{ nm}$) with and without 10 mM NaCl at (A) pH 6.3 and (B) pH 4.5. Reaction conditions: catalyst, 0.3 g; reaction solution, 400 mL; light source, high-pressure mercury lamp (450 W); reaction vessel, Pyrex inner-irradiation vessel with aqueous NaNO_2 solution filter. Solid circles, H_2 without NaCl; open circles, O_2 without NaCl; solid squares, H_2 with 10 mM NaCl; open squares, O_2 with 10 mM NaCl.

that achieved in the HCl-adjusted solution (H_2 , $166 \mu\text{mol h}^{-1}$; O_2 , $83 \mu\text{mol h}^{-1}$), suggesting that Na^+ has a positive effect on activity.

The effects of Na^+ on activity was further examined without interference from Cl^- by conducting reactions using Na_2SO_4 . The dependence of the rates of H_2 and O_2 evolution in overall water splitting using $\text{Rh}_{2-y}\text{Cr}_y\text{O}_3$ -loaded $(\text{Ga}_{1-x}\text{Zn}_x)(\text{N}_{1-x}\text{O}_x)$ under visible light on the concentration of Na_2SO_4 in the reactant solution is shown in Fig. 4. As in the case for NaCl (Fig. 1), the activity increased with increasing Na_2SO_4 concentration to a maximum at 5 mM (corresponding to 10 mM Na^+), then decreased with further Na_2SO_4 addition to a relatively constant level at concentrations of 50 mM or higher. The evolution ratio of H_2 to O_2 remained close to stoichiometric ($\text{H}_2/\text{O}_2 \approx 2$) even at high concentrations of Na_2SO_4 (over 100 mM). This behavior is clearly different from that observed using NaCl (Fig. 1). The degree of activity suppression with increasing Na_2SO_4 concentration is also smaller than for NaCl, maintaining at least 75% of the original activity even in the presence of up to 500 mM Na_2SO_4 . In contrast, the same catalyst was deactivated by 60–65% in the presence of just 60 mM NaCl. The promotional effect of Na^+ on the activity of $\text{Rh}_{2-y}\text{Cr}_y\text{O}_3$ -loaded

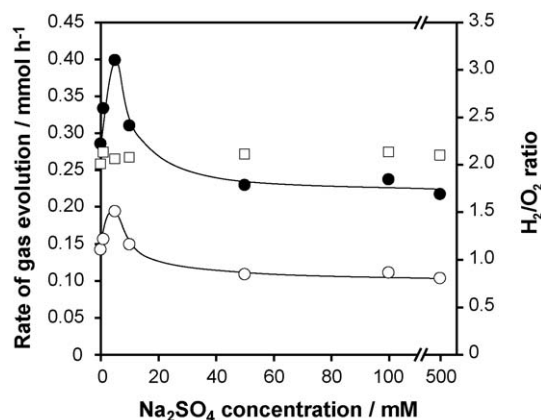


Fig. 4. Dependence of rate of H_2 and O_2 evolution in overall water splitting using $\text{Rh}_{2-y}\text{Cr}_y\text{O}_3$ -loaded $(\text{Ga}_{1-x}\text{Zn}_x)(\text{N}_{1-x}\text{O}_x)$ under visible light ($\lambda > 400 \text{ nm}$) on Na_2SO_4 concentration. Reaction conditions: catalyst, 0.3 g; reaction solution, 400 mL; light source, high-pressure mercury lamp (450 W); reaction vessel, Pyrex inner-irradiation vessel with aqueous NaNO_2 solution filter. Solid circles, H_2 ; open circles, O_2 ; open squares, H_2/O_2 evolution ratio.

Table 2

Photocatalytic activities of Rh_{2–y}Cr_yO₃-loaded (Ga_{1–x}Zn_x)(N_{1–x}O_x) for overall water splitting under visible light ($\lambda > 400$ nm) in the presence of various metal chlorides^a.

Entry	Chloride	Activity ^b ($\mu\text{mol h}^{-1}$)	
		H ₂	O ₂
1	HCl ^c	166	83
2	LiCl	268	128
3	NaCl	278	132
4	KCl	270	129
5	RbCl	181	85
6	CsCl	221	104
7	MgCl ₂	189	85
8	CaCl ₂	215	98
9	SrCl ₂	224	102
10	BaCl ₂	251	114

^a Reaction conditions: catalyst, 0.3 g; reaction solution, aqueous solution (400 mL, pH 4.5); light source, high-pressure mercury lamp (450 W); reaction vessel, Pyrex inner-irradiation vessel with aqueous NaNO₂ solution filter.

^b Average rate of gas evolution for 5 h.

^c The concentration of Cl[–] is about 0.03 mM.

(Ga_{1–x}Zn_x)(N_{1–x}O_x) for overall water splitting was thus clearly observed, even with only a small amount of Na₂SO₄ (≤ 5 mM) added to the reactant solution.

3.3. Effect of cations on activity

Table 2 summarizes the rates of H₂ and O₂ evolution from aqueous solutions containing various alkaline- or alkaline earth-metal chlorides (10 mM) at pH 4.5 for Rh_{2–y}Cr_yO₃-loaded (Ga_{1–x}Zn_x)(N_{1–x}O_x) under visible light ($\lambda > 400$ nm). When the reaction was performed in the presence of alkaline chlorides, the evolution of both H₂ and O₂ was observed, although the ratio of evolved H₂ to O₂ (H₂/O₂ \approx 2.1) deviated slightly from that expected from the stoichiometry in all cases. Although no distinct relationship between alkaline metals and activity was observed, the activities were higher than that achieved in aqueous HCl solution containing no alkaline metal cations (entry 1) and tended to become lower with increasing atomic number of the alkaline metal. Using alkaline earth-metal chlorides as additives, H₂ and O₂ were both evolved at higher rates than observed in aqueous HCl solution (entry 1), as observed for the alkaline chlorides. In contrast to the alkaline chloride cases, however, the activities achieved using alkaline earth-metal chlorides increased gradually with increasing atomic number of the alkaline earth-metals. Deviation from stoichiometry was also observed in this case (H₂/O₂ \approx 2.2), and the deviation was larger than that observed using alkaline metal chlorides (H₂/O₂ \approx 2.1), primarily attributable to the higher concentration of Cl[–] in the alkaline earth-chlorides. As indicated in Fig. 1, the probability that photooxidation of Cl[–] by valence band holes takes place rises with increasing Cl[–] concentration in the reactant solution. On the basis of these results, it is clear that the negative effect of Cl[–] on activity is compensated by the coexistence of alkaline- or alkaline earth-metal cations in the reactant solution, and that the photocatalytic activity of Rh_{2–y}Cr_yO₃-loaded (Ga_{1–x}Zn_x)(N_{1–x}O_x) is affected by the kind of metal cation present in the reactant solution.

Among the chlorides examined, the addition of an appropriate amount of lithium, sodium, or potassium chloride (LiCl, NaCl, KCl) to the reactant solution resulted in the most marked increasing in activity for overall water splitting (Table 2). The effect of lithium, sodium, and potassium on these reactions was thus further examined by conducting reactions using the corresponding sulfates (Li₂SO₄, Na₂SO₄, K₂SO₄). Table 3 lists the photocatalytic activities of Rh_{2–y}Cr_yO₃-loaded (Ga_{1–x}Zn_x)(N_{1–x}O_x) for overall

water splitting under visible light ($\lambda > 400$ nm) in the presence of these sulfates at pH 4.5 (adjusted with H₂SO₄) and ca. 6.0. The concentration of sulfates was fixed at 5 mM, at which the highest activity was obtained in the case of Na₂SO₄ (Fig. 4). In all cases, nearly stoichiometric H₂ and O₂ evolution was observed, indicating that overall water splitting proceeded. At pH 4.5, the activities achieved in the presence of Li₂SO₄ (entry 2) and K₂SO₄ (entry 4) were lower than those achieved without additives (entry 1) and in the presence of Na₂SO₄ (entry 3). These results differ from those obtained for the corresponding chlorides. At neutral pH, the activities for H₂ and O₂ evolution were improved by 50–70% upon addition of any of these three sulfates (entries 6–8). The promotional effect of metal cations on activity thus appears to be dependent on the counter anion species and pH of the reactant solution.

Interactions at the interface between the photocatalyst and the electrolyte solution will undoubtedly be complex and difficult to observe using the present experimental setup. However, it is considered that the addition of electrolytes, particularly NaCl and Na₂SO₄, to the reactant solution may facilitate surface redox reactions and/or compensate for the detrimental effect of surface defects that can act as recombination centers between photogenerated electrons and holes, thereby enhancing activity. Similar promotional effects on photocatalytic activity for overall water splitting by electrolyte addition have been observed for other UV-active metal-oxide photocatalysts, although the mechanism for such an effect has not been reported in any detail [5,25].

3.4. Direct splitting of seawater under visible light

On the basis of the results above, it is expected that Rh_{2–y}Cr_yO₃-loaded (Ga_{1–x}Zn_x)(N_{1–x}O_x) will catalyze the splitting of seawater under visible light to produce H₂ and O₂. Seawater splitting reactions were attempted in the present study using artificially prepared seawater (see Section 2) containing approximately 500 mM Cl[–]. A time course of H₂ and O₂ evolution from seawater (pH 8.0) using Rh_{2–y}Cr_yO₃-loaded (Ga_{1–x}Zn_x)(N_{1–x}O_x) under visible light ($\lambda > 400$ nm) is shown in Fig. 5. The data for the corresponding pure water reaction (pH 6.3) is shown for comparison. As reported previously, Rh_{2–y}Cr_yO₃-loaded (Ga_{1–x}Zn_x)(N_{1–x}O_x) catalyzes steady and stoichiometric H₂ and O₂ evolution from pure water, although the activity decreases after an extended reaction period (longer than 24 h) [14]. The catalyst was also found to be active for seawater splitting to produce H₂ and O₂. The activity for seawater splitting was lower than that achieved from pure water, and the rates of H₂ and O₂ evolution from seawater decreased gradually from the

Table 3

Photocatalytic activities of Rh_{2–y}Cr_yO₃-loaded (Ga_{1–x}Zn_x)(N_{1–x}O_x) for overall water splitting under visible light ($\lambda > 400$ nm) in the presence of A₂SO₄ (A = Li, Na, or K)^a.

Entry	Alkaline sulfate ^b	pH	Activity ^c ($\mu\text{mol h}^{-1}$)	
			H ₂	O ₂
1	None	4.5	264	132
2	Li ₂ SO ₄	4.5	217	109
3	Na ₂ SO ₄	4.5	399	193
4	K ₂ SO ₄	4.5	257	121
5	None	6.2	285	142
6	Li ₂ SO ₄	5.7	485	242
7	Na ₂ SO ₄	5.8	395	192
8	K ₂ SO ₄	5.8	501	251

^a Reaction conditions: catalyst, 0.3 g; reaction solution, aqueous solution (400 mL); light source, high-pressure mercury lamp (450 W); reaction vessel, Pyrex inner-irradiation vessel with aqueous NaNO₂ solution filter.

^b Concentration, 5 mM.

^c Average rate of gas evolution for 5 h.

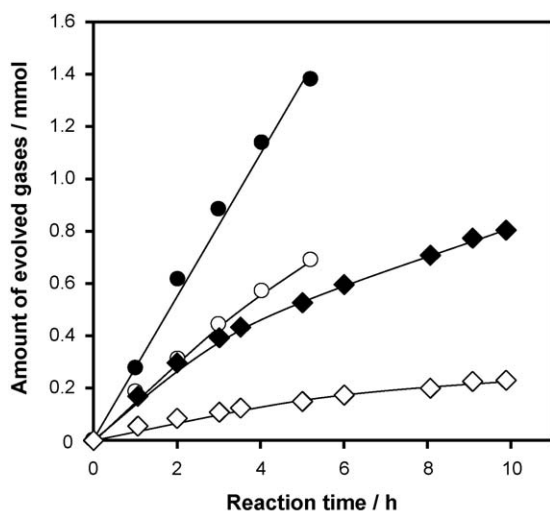


Fig. 5. Time courses of H₂ and O₂ evolution using Rh_{2-y}Cr_yO₃-loaded (Ga_{1-x}Zn_x)(N_{1-x}O_x) under visible light ($\lambda > 400$ nm). Reaction conditions: catalyst, 0.3 g; reaction solution, 400 mL; light source, high-pressure mercury lamp (450 W); reaction vessel, Pyrex inner-irradiation vessel with aqueous NaNO₂ solution filter. Solid circles, H₂ from pure water (pH 6.3); open circles, O₂ from pure water (pH 6.3); solid squares, H₂ from artificial seawater (pH 8.0); open squares, O₂ from artificial seawater (pH 8.0).

beginning of the reaction. The ratio of produced H₂ to O₂ was approximately 3, substantially higher than that expected from stoichiometry. The degradation of catalytic activity in seawater is considered to be primarily due to the hydrolysis of (Ga_{1-x}Zn_x)(N_{1-x}O_x) at such basic pH (8.0). The surface of gallium-based (oxy)nitrides is known to be inherently unstable in basic media [14,26]. The non-stoichiometric H₂ and O₂ evolution is attributable to the oxidation of adsorbed Cl⁻ by a fraction of the holes generated in the valence band of (Ga_{1-x}Zn_x)(N_{1-x}O_x), as discussed above. Although photoelectrochemical measurements using a porous (Ga_{1-x}Zn_x)(N_{1-x}O_x) electrode have indicated that the oxidation of I⁻ occurs more readily on the (Ga_{1-x}Zn_x)(N_{1-x}O_x) surface than the photooxidation of water [27], the concentration of I⁻ in the artificial seawater is very low (ca. 0.6 μ M, corresponding to 0.24 μ mol I⁻) and hence the effect appears to be very small. It is thus concluded that the main culprit of the decreased activity in seawater is Cl⁻ that suppresses water oxidation and may induce other side reactions, thereby contributing to a decrease in overall water splitting efficiency of Rh_{2-y}Cr_yO₃-loaded (Ga_{1-x}Zn_x)(N_{1-x}O_x).

4. Conclusion

Photocatalytic overall water splitting using (Ga_{1-x}Zn_x)(N_{1-x}O_x) catalyst in the presence of various electrolytes under visible light ($\lambda > 400$ nm) were examined. The catalytic behavior was found to differ according to the cocatalyst and pH-adjusting reagent employed. Rh_{2-y}Cr_yO₃ cocatalysts-loaded on (Ga_{1-x}Zn_x)(N_{1-x}O_x) promote H₂ evolution with high selectivity even in the presence of electron acceptors such as NO₃⁻ and O₂ that can hinder reduction of H⁺, while RuO₂ cocatalysts improve both water reduction and oxidation in overall water splitting by (Ga_{1-x}Zn_x)(N_{1-x}O_x). The addition of an appropriate amount of electrolyte (e.g., NaCl and

Na₂SO₄) to the reactant solution was shown to enhance overall water splitting using Rh_{2-y}Cr_yO₃-loaded (Ga_{1-x}Zn_x)(N_{1-x}O_x). The same catalyst was also demonstrated to successfully split artificial seawater under visible light, although at activity approximately half that achieved from pure water and at a substantial deviation from the stoichiometric evolution ratio. Nevertheless, the present results demonstrate the possibility of realizing a seawater-based reaction system for photocatalytic overall water splitting under visible light. It is expected that with appropriate treatment of the catalyst and/or reaction system that more efficient splitting of seawater will be achievable.

Acknowledgements

This work was supported by the Research and Development in a New Interdisciplinary Field Based on Nanotechnology and Materials Science program of the Ministry of Education, Culture, Sports, Science and Technology (MEXT) of Japan. Acknowledgement is extended to Tokyo Metropolitan Collaboration of Regional Entities for the Advancement of Technological Excellence, Japan Science and Technology Agency (JST). One of the authors (K.M.) is supported by a Fellowship from the Japan Society for the Promotion of Science (JSPS).

References

- [1] A. Kudo, H. Kato, I. Tsuji, *Chem. Lett.* 33 (2004) 1534.
- [2] J.S. Lee, *Catal. Surv. Asia* 9 (2005) 217.
- [3] P.G. Hoertz, T.E. Mallouk, *Inorg. Chem.* 44 (2005) 6828.
- [4] K. Maeda, K. Domen, *J. Phys. Chem. C* 111 (2007) 7851.
- [5] S.M. Ji, H. Jun, J.S. Jang, H.C. Son, P.H. Borse, J.S. Lee, *J. Photochem. Photobiol. A: Chem.* 189 (2007) 141.
- [6] K. Maeda, T. Takata, M. Hara, N. Saito, Y. Inoue, H. Kobayashi, K. Domen, *J. Am. Chem. Soc.* 127 (2005) 8286.
- [7] K. Maeda, K. Teramura, T. Takata, M. Hara, N. Saito, K. Toda, Y. Inoue, H. Kobayashi, K. Domen, *J. Phys. Chem. B* 109 (2005) 20504.
- [8] K. Teramura, K. Maeda, T. Saito, T. Takata, N. Saito, Y. Inoue, K. Domen, *J. Phys. Chem. B* 109 (2005) 21915.
- [9] K. Maeda, K. Teramura, D. Lu, T. Takata, N. Saito, Y. Inoue, K. Domen, *Nature* 440 (2006) 295.
- [10] K. Maeda, K. Teramura, N. Saito, Y. Inoue, K. Domen, *J. Catal.* 243 (2006) 303.
- [11] K. Maeda, K. Teramura, D. Lu, T. Takata, N. Saito, Y. Inoue, K. Domen, *J. Phys. Chem. B* 110 (2006) 13753.
- [12] K. Maeda, K. Teramura, D. Lu, N. Saito, Y. Inoue, K. Domen, *Angew. Chem. Int. Ed.* 45 (2006) 7806.
- [13] K. Maeda, K. Teramura, D. Lu, N. Saito, Y. Inoue, K. Domen, *J. Phys. Chem. C* 111 (2007) 7554.
- [14] K. Maeda, K. Teramura, H. Masuda, T. Takata, N. Saito, Y. Inoue, K. Domen, *J. Phys. Chem. B* 110 (2006) 13107.
- [15] H. Hashiguchi, K. Maeda, R. Abe, A. Ishikawa, J. Kubota, K. Domen, submitted for publication.
- [16] J.A. Dean, *Lange's Handbook of Chemistry*, 13th edition, McGraw-Hill, New York, 1985.
- [17] H. Kato, A. Kudo, *Phys. Chem. Chem. Phys.* 4 (2002) 2833.
- [18] M. Abdullah, G.K.C. Low, R.W. Matthews, *J. Phys. Chem.* 94 (1990) 6820.
- [19] D. Chen, A.K. Ray, *Water Res.* 32 (1998) 3223.
- [20] K. Kalyanasundaram, M. Grätzel, *Angew. Chem. Int. Ed.* 18 (1979) 701.
- [21] T. Kawai, T. Sakata, *Nature* 286 (1980) 474.
- [22] E. Borgarello, J. Kiwi, E. Pelizzetti, M. Visca, M. Grätzel, *Nature* 289 (1981) 158.
- [23] A. Harriman, I.J. Pickering, J.M. Thomas, P.A. Christensen, *J. Chem. Soc., Faraday Trans. 1* (84) (1988) 2795.
- [24] Y. Lee, K. Teramura, M. Hara, K. Domen, *Chem. Mater.* 19 (2007) 2120.
- [25] K. Sayama, H. Arakawa, *J. Photochem. Photobiol. A: Chem.* 94 (1996) 67.
- [26] K. Fujii, K. Kusakabe, K. Ohkawa, *Jpn. J. Appl. Phys.* 44 (2005) 7433.
- [27] K. Maeda, H. Hashiguchi, H. Masuda, R. Abe, K. Domen, *J. Phys. Chem. C* 112 (2008) 3447.